^{15}N Chemical Shielding in Glycyl Tripeptides: Measurement by Solid-State NMR and Correlation with X-ray Structure

Eduard Y. Chekmenev, Qianwen Zhang,† Kevin W. Waddell, Mark S. Mashuta, and Richard J. Wittebort*

Contribution from the Department of Chemistry, 2320 South Brook Street, University of Louisville, Louisville, Kentucky 40292

Received July 2, 2003; E-mail: rjwitt01@athena.louisville.edu

Abstract: ^{15}N chemical shielding parameters are reported for central glycyl residues in crystallographically characterized tripeptides with α-helix, β-strand, polyglycine II (3_1-helix), and extended structures. Accurate values of the shielding components (2−5 ppm) are determined from MAS and stationary spectra of peptides containing [2-^{13}C,^{15}N]Gly. Two dipolar couplings, ^{1}H−^{15}N and ^{13}Cα−^{15}N, are used to examine ^{15}N shielding tensor orientations in the molecular frame and the results indicate that the δ_{11}, δ_{33} plane of the shielding tensor is not coincident with the peptide plane. The observed isotropic shifts, which vary over a range of 13 ppm, depend on hydrogen bonding (direct and indirect) and local conformation. Tensor spans, $\delta_{span} = \delta_{11} - \delta_{33}$, and their deviations from axial symmetry, $\delta_{dev} = \delta_{22} - \delta_{33}$, vary over a larger range and are grouped according to 2° structure. Augmented by previously reported ^{13}Cα shielding parameters, a prediction scheme for the 2° structure of glycyl residues in proteins based on shielding parameters is proposed.

Introduction

^{15}N is an essential nucleus in solution and solid-state NMR studies of biomolecules. It has a key location in the polypeptide backbone; dispersion of isotropic shifts is large, and their systematic variation with 2° structure, side chain conformation and local H-bonding[1,2] is now used in structure determination. The full chemical shielding tensor is also central to a wide variety of solution and solid-state experiments. An example from solution NMR is the study of molecular dynamics using ^{15}N relaxation. The accuracy with which these experiments are analyzed is limited by knowledge of ^{15}N shielding tensors, and it has been indicated that the tensors typically used in solution NMR studies are systematically larger than those determined by solid-state NMR spectroscopy.[3] Other examples from solution NMR are the choice of optimum field strength for studies using the TROSY method and obtaining structural constraints from residual anisotropic chemical shifts in partially oriented samples. An example from solid-state NMR is the PISEMA experiment used to determine membrane protein structures in oriented membranes.[4−6] If the shielding tensor principal components and their molecular orientation are known, peptide plane orientations can be determined from the 2-D correlation of ^{15}N chemical shift and ^{15}N−^{1}H dipolar coupling. Analogous to solution

structure determination based on isotropic shifts, solid-state methods for 2° structure determination based on ^{13}Cα shielding principal components have been discussed.[7−10] Typically, principal components vary over a larger range than isotropic shifts,[7,9] and it would be useful to augment ^{13}Cα with ^{15}N shielding parameters to provide additional structural constraints and resolve ambiguities.

The number of experimentally determined ^{15}N shielding tensors is small compared to the large database of isotropic shifts in proteins of known structure. While the latter has been carefully analyzed, the connection of the former with structure is more direct since individual tensor components, as opposed to their average, are observed and each has a well-defined molecular orientation. Accordingly, it is useful to summarize what is currently known about peptide ^{15}N shielding. The initial benchmark for the magnitude and orientation of peptide ^{15}N shielding tensors is the single-crystal study of gly-gly·HCl.[11] The amide nitrogen has a span, $\delta_{span} = \delta_{11} - \delta_{33}$, of 155 ppm and vanishing deviation from axial symmetry, $\delta_{dev} = \delta_{22} - \delta_{33}$. The unique component, δ_{11}, is the most deshielded and lies in the peptide plane rotated 21° from the N−H bond toward C′ of the same amide group.

From studies of peptides of the form Ac-Gly-X-NH$_2$, it was concluded that there is no single amide shielding tensor.[12,13]

† Current address: Tecmag Corp., 6006 Bellaire Blvd., Houston, TX 77081.
(1) Wishart, D. S.; Case, D. A. *Methods. Enzymol.* **2001**, *338*, 3−34.
(2) Wishart, D. S.; Nip, A. M. *Biochem. Cell Biol.* **1998**, *76*, 153−163.
(3) Cornilescu, G.; Bax, A. *J. Am. Chem. Soc.* **2000**, *122*, 10143−10154.
(4) Tian, C. L.; Tobler, K.; Lamb, R. A.; Pinto, L. H.; Cross, T. A. *Biochemistry* **2002**, *41*, 11294−11300.
(5) Opella, S. J.; Nevzorov, A.; Mesleh, M. F.; Marassi, F. M. *Biochem. Cell Biol.* **2002**, *80*, 597−604.
(6) Ramamoorthy, A.; Wu, C. H.; Opella, S. J. *J. Magn. Reson.* **1999**, *140*, 131−140.

(7) Havlin, R. H.; Laws, D. D.; Bitter, H. M.; Sanders, L. K.; Sun, H.; Grimley, J. S.; Wemmer, D. E.; Pines, A.; Oldfield, E. *J. Am. Chem. Soc.* **2001**, *123*, 10362−10369.
(8) Heller, J.; Laws, D. D.; Tomaselli, M.; King, D. S.; Wemmer, D. E.; Pines, A.; Havlin, R. H.; Oldfield, E. *J. Am. Chem. Soc.* **1997**, *119*, 7827−7831.
(9) Chekmenev, E. Y.; Xu, R. Z.; Mashuta, M. S.; Wittebort, R. J. *J. Am. Chem. Soc.* **2002**, *124*, 11894−11899.
(10) Hong, M. *J. Am. Chem. Soc.* **2000**, *122*, 3762−3770.
(11) Harbison, G. S.; Jelinski, L. W.; Stark, R. E.; Torchia, D. A.; Herzfeld, J.; Griffin, R. G. *J. Magn. Reson.* **1984**, *60*, 79−82.

The central amide linkage in these peptides (X = ala or gly, respectively) have substantial deviations from axial symmetry, δ_{dev} = 24 or 41 ppm, and large spans, 170 or 185 ppm, respectively. Tensor orientations were examined using the $^{13}C'$–^{15}N dipolar couplings and found to be similar to that in gly-gly·HCl (δ_{11} is 20° from the N–H bond).[12,13] With the symmetry based assumption that δ_{11} and δ_{33} should lie approximately in the molecular plane, δ_{22} was identified as the component close to the peptide plane normal. More recently, observation of the ^{15}N–^1H dipolar coupling in *N*-acetylglycine indicates that δ_{33} can be out of the plane.[14]

Not surprisingly, the imide nitrogen in ala-pro has substantially different shielding parameters. Both δ_{span} and δ_{dev} are large, 197 and 101 ppm, respectively. However, the orientation of the downfield component is, within a few degrees, the same as that described above.[15] The val$_6$ residue of gramicidin, with δ_{span} = 165 ppm and δ_{dev} = 25 ppm,[16] suggests that the effect of amino acid type, proline aside, is in the range seen for gly residues.

Conformation is an important factor in ^{15}N shielding. Compared to gly-gly·HCl, zwitterionic gly-gly·H$_2$O has a different crystal conformation and its shielding parameters are larger, δ_{span} = 175.5 ppm and δ_{dev} = 30.5 ppm.[17] This is further established with the nonionic peptide Boc-gly-gly-[^{15}N]gly benzyl ester which crystallizes in monoclinic and triclinic forms.[18] An X-ray structure was determined only for the monoclinic form, but both have H-bonded amides and different spans, 168 or 184 ppm, and deviations from axial symmetry, 7 and 47 ppm.[18] Glycyl ^{15}N principal components in homopolypeptides adopting helical or sheet conformations show a consistently larger δ_{dev} for sheets.[14] More recently, [^{15}N]gly shielding parameters in several peptides of known conformation were reported and interpreted in terms of H-bond distances.[19] We note that the peptides with β-strand torsion angles at the labeled gly position have similar shielding parameters, $\delta_{span} \approx 181$ ppm and $\delta_{dev} \approx 39$ ppm, which are larger than the single example with an α-helix like conformation, δ_{span} = 161 ppm and δ_{dev} = 15 ppm. A similar dependence of tensor parameters on 2° structure was reported in NMR studies of weakly oriented ubiquitin[3] wherein a projection of the shielding tensor is observed for each amide nitrogen. Although complete, site-specific determination of shielding tensors for each amide group was not determined, these results also indicate larger average δ_{span} and δ_{dev} for β-sheet residues.

The effects of conformation and H-bonding on ^{15}N amide shielding and isotropic shifts have also been studied theoretically.[20–24] Changes in tensor components at the central amide

in *N*-formyl-gly-gly amide are predominantly affected (~20 ppm) by the nearest torsion angles, ψ_{i-1} and ϕ_i, with smaller changes (~8 ppm) dependent on ϕ_{i-1} and ψ_i. Compared to empirical conformational surfaces of isotropic shifts as a function of ψ_{i-1} and ϕ_i,[2] theoretical predictions are similar but quantitatively larger.[22] This difference is potentially due to neglect of other properties in the statistical analysis (ϕ_{i-1}, ψ_i, and H-bonding, for example) or the fact that ab initio calculations are frequently scaled down to better compare with experiment.[7] Extensive DFT calculations of isotropic shifts[21] in longer α-helices and β-sheets indicate a similar hierarchy of effects with an important addition. The direct H-bond to the amide nitrogen has a larger downfield shift in helix (~3.7 ppm) than sheet residues (~1.2 ppm), and for both, the effect of an indirect H-bond at C=O is larger than the direct H-bond.

In this paper, we present a systematic experimental investigation of glycyl ^{15}N peptide shielding. The available evidence indicates that the properties that determine shielding in peptides and small fragments are entirely relevant to proteins.[7,9] While a complete study would include all amino acids, the peptides studied here contain [2-^{13}C,^{15}N]gly at the central residue and have torsion angles representing helix, sheet, and polyglycine II type conformations. Importantly, a high resolution X-ray structure has been previously determined or is reported here for each peptide. Thus, relevant structural features such as backbone and side chain torsion angles and H-bond distances are known with better precision than in either protein X-ray or solution NMR structures. Previously, we have examined most of the peptides studied here by ^{13}C NMR.[9] Additions in the current study include two polymorphs of GGG, new polymorphs of AGG and GGV, and the peptide GGF. Consequently, ^{15}N shielding values are reported for GGG in four forms and GGV and AGG in two forms with distinct conformations and H-bonding arrangements. Three aspects of ^{15}N shielding are examined. First, we examine the extent of internal motion in the solid state by determining shielding parameters at −123 °C and 20 °C for a peptide with a representative crystallographic *R* factor (0.054). Second, the molecular orientations of the principal components are studied in GGV and VGG using both dipolar couplings available in the double-labeled peptides. As summarized above, our current knowledge of peptide nitrogen tensor orientations is based on the single-crystal study of gly-gly·HCl and a small number of powder sample studies using one dipole coupling ($^{13}C'$–^{15}N, ^{15}N–^1H or ^{15}N–^2H). For either of two reasons, these results do not provide a complete picture of the shielding tensor orientation. In the single-crystal study, the tensor is nearly axially symmetric and only the orientation of the unique axis, δ_{11}, could be determined, while, in the powder sample experiments, the dipole coupled spectrum is invariant to an arbitrary rotation of the shielding tensor about the dipole–dipole vector.[12] With double-labeled samples, we orient the shielding tensor relative to the ^{15}N–^1H bond (by applying Lee–Goldburg ^1H decoupling[14]) and relative to the ^{15}N–$^{13}C\alpha$ bond (by applying only ^1H decoupling). Combined, these experiments reduce the tensor orientation to two possibilities and confirm that both δ_{11} and δ_{33} can lie out of the peptide plane, albeit by a small amount. Finally, principal

(12) Oas, T. G.; Hartzell, C. J.; Dahlquist, F. W.; Drobny, G. P. *J. Am. Chem. Soc.* **1987**, *109*, 5962−5966.
(13) Hartzell, C. J.; Whitfield, M.; Oas, T. G.; Drobny, G. P. *J. Am. Chem. Soc.* **1987**, *109*, 5966−5969.
(14) Lee, D. K.; Wittebort, R. J.; Ramamoorthy, A. *J. Am. Chem. Soc.* **1998**, *120*, 8868−8874.
(15) Valentine, K. G.; Rockwell, A. L.; Gierasch, L. M.; Opella, S. J. *J. Magn. Reson.* **1987**, *73*, 519−523.
(16) Wang, C.; Teng, Q.; Cross, T. A. *Biophys. J.* **1992**, *61*, 1550−1556.
(17) Roberts, J. E.; Harbison, G. S.; Munowitz, M. G.; Herzfeld, J.; Griffin, R. G. *J. Am. Chem. Soc.* **1987**, *109*, 4163−4169.
(18) Hiyama, Y.; Niu, C. H.; Silverton, J. V.; Bavoso, A.; Torchia, D. A. *J. Am. Chem. Soc.* **1988**, *110*, 2378−2383.
(19) Fukutani, A.; Naito, A.; Tuzi, S.; Saito, H. *J. Mol. Struct.* **2002**, *602−603*, 491−503.
(20) Xu, X. P.; Case, D. A. *J. Biomol. NMR* **2001**, *21*, 321−333.
(21) Xu, X. P.; Case, D. A. *Biopolymers* **2002**, *65*, 408−423.
(22) Le, H. B.; Oldfield, E. *J. Phys. Chem.* **1996**, *100*, 16423−16428.
(23) Walling, A. E.; Pargas, R. E.; deDios, A. C. *J. Phys. Chem. A* **1997**, *101*, 7299−7303.
(24) Luman, N. R.; King, M. P.; Augspurger, J. D. *J. Comput. Chem.* **2001**, *22*, 366−372.

shielding components are reported for the complete set of peptides. Isotropic chemical shifts have a substantial range and are systematically analyzed in terms of structural features used in the analysis of protein ^{15}N shifts; direct and indirect H-bonding of the amide group, preceding residue type and ψ_{i-1}, ϕ_i, χ_{i-1} torsions. Examination of the shielding tensor spans and deviations from axial symmetry shows that both are grouped according to 2° structure.

Experimental Methods

Peptide Samples. Methods used for peptide synthesis and characterization by X-ray crystallography have been described previously.[9] In addition to peptides previously studied, additional polymorphs of G*GG[25,26] and G*GF[27] were prepared for the present study using the same methods.

NMR Spectra. ^{15}N NMR spectra were obtained on a home-built 11.7 T instrument (^{15}N Larmor frequency of 50.2 MHz) with a 4 mm (^{1}H/^{13}C/^{15}N) triple-resonance MAS probe built on a design previously described.[28] Sample spinning speeds were controlled to within ±3 Hz (Doty Scientific, Columbia, S.C.). ^{15}N spectra were excited by cross-polarization from abundant protons using a 1−3 ms Hartman−Hahn contact ($\gamma B_1^N/2\pi = \gamma B_1^H/2\pi = 40$ kHz) and accumulated with high power ($\gamma B_1^H/2\pi = 125$ kHz) two pulse phase modulated (tppm) decoupling[29] with recycle times sufficiently long to give equilibrium signal intensities. The tppm phase shift was 22.5°, and line widths were minimized by adjusting the ^{1}H flip angle (~150°). Spectra with scaled ^{1}H dipolar coupling were obtained by simultaneous application of ^{13}C and off-resonant Lee−Goldburg ^{1}H decoupling.[30] All spectra were referenced to external solid ammonium chloride[31] and then converted to the liquid ammonia scale[32] using δ_{iso}(^{15}NH$_4$Cl, solid) = 39.1 ppm. A typical sample size was 10−20 mg of peptide, spectra were accumulated with 1024 transients, and data were processed with 25 Hz Gaussian broadening.

X-ray Structures. Structures of the hydrogen chloride salts of AGG and GGV have not previously been reported and are given here. Both structures were determined at 100 K on a Bruker SMART APEX CCD diffractometer. A small (0.12 × 0.09 × 0.05 mm^3) colorless single crystal of AGG·HCl (CCDC code 213476) was mounted on a kryoloop with Paratone oil for data collection. A total of 1868 30 s frame ω-scan exposures of data were acquired to a 2θ max = 56.44° using monochromated Mo K radiation (0.710 73 Å).[33] Frame data were processed[34] to determine final unit cell parameters ($a = 5.2258(5)$ Å, $b = 8.7007(9)$ Å, $c = 22.970(18)$ Å, $\alpha = \beta = \gamma = 90°$, $V = 1044.42$-(18) Å^3, $Z = 4$, $\rho_{calcd} = 1.524$ mg m^{-3}) and produced 8593 raw reflections that were corrected for absorption (transmission min/max = 0.795/0.987; $\mu = 0.366$ mm^{-1}).[35] The structure was solved by direct methods in the noncentrosymmetric orthorhombic space group $P2_12_12_1$ using SHELXS-90[36] and refined by least-squares methods on F^2 using SHELXL-97[37] incorporated into the SHELXTL (v. 6.12)[38] suite of programs. All non-hydrogen atoms were refined anisotropically.
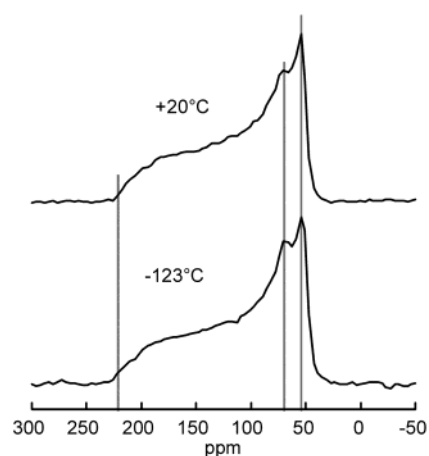
(25) Meuleman, R.; Piret, P.; Vanmeers, M. *Acta Crystallogr., Sect. B* **1971**, *B 27*, 1187−1190.
(26) Van der Helm, D.; Willoughby, T. V. *Acta Crystallogr., Sect. B* **1969**, *B25*, 2317−2326.
(27) Murali, R.; Subramanian, E. *Int. J. Pept. Protein Res.* **1987**, *29*, 374−380.
(28) Zhang, Q. W.; Zhang, H.; Lakshmi, K. V.; Lee, D. K.; Bradley, C. H.; Wittebort, R. J. *J. Magn. Reson.* **1998**, *132*, 167−171.
(29) Bennett, A. E.; Rienstra, C. M.; Auger, M.; Lakshmi, K. V.; Griffin, R. G. *J. Chem. Phys.* **1995**, *103*, 6951−6958.
(30) Lee, M.; Goldburg, W. I. *Phys. Rev.* **1965**, *140A*, 1261−1271.
(31) Hayashi, S.; Hayamizu, K. *Bull. Chem. Soc. Jpn.* **1991**, *64*, 688−690.
(32) Levy, G. C.; Lichter, R. L. *Nitrogen-15 Nuclear Magnetic Spectroscopy*; John Wiley & Sons: New York, 1979.
(33) *SMART*, version 5.625; Bruker Advanced X-ray Solutions, Inc.: Madison, WI, 2001.
(34) *SAINT*, version 6.22; Bruker Advanced X-ray Solutions, Inc.: Madison, WI, 2001.
(35) Sheldrick, G. M. *SADABS*, version 2.02; *Area Detector Absorption Correction*; University Göttingen: Göttingen, Germany, 1997.
(36) Sheldrick, G. M. *Acta Crystallogr., Sect. A* **1990**, *46*, 467−473.

Figure 1. ^{13}C coupled ^{15}N spectrum of AGG acquired at −123 °C and 20 °C. Within spectral resolution (4 ppm), all spectral features including the overall breadth are unchanged upon changing the temperature by 143 °C.

Hydrogen atoms of the terminal amine, both amide groups, and the carboxylic acid were located by electron difference maps and refined isotropically. Methyl and methylene hydrogen atoms were placed in their geometrically generated positions and refined as riding models. For all 2214 unique reflections (R(int) = 0.048), the final anisotropic full matrix least-squares refinement on F^2 for 165 variables converged at R1 = 0.053 and wR2 = 0.109 with a GOF of 1.05 and 0.416e Å^{-3} residual. The absolute structure was determined by refinement of the Flack parameter (0.07(1)). X-ray structural analysis for GGV·HCl (CCDC code 213477) was preformed on a 0.33 × 0.14 × 0.06 mm^3 colorless needle using an identical data acquisition strategy described above to a 2θ max = 56.42°. GGV·HCl crystallizes in the space group $P2_12_12_1$ with the following unit cell parameters: $a = 6.9890(8)$ Å, $b = 8.2684(10)$ Å, $c = 21.834(3)$ Å, $\alpha = \beta = \gamma = 90°$, $V = 1261.8(3)$ Å^3, $Z = 4$, and $\rho_{calcd} = 1.409$ mg m^{-3}. The 11 002 raw reflections were corrected for absorption (transmission min/max = 0.951/0.980; $\mu = 0.311$ mm^{-1}), and the structure was solved by direct methods and refined on F^2 using SHELXTL. All non-hydrogen atoms were refined anisotropically. All hydrogen atoms were located by electron difference maps and refined isotropically. For all 2931 unique reflections (R(int) = 0.0263), the final anisotropic full matrix least-squares refinement on F^2 for 184 variables converged at R1 = 0.027 and wR2 = 0.055 with a GOF of 1.01 and 0.277e Å^{-3} residual. The absolute structure was determined by refinement of the Flack parameter 0.03(4). Selected bond distance and angles involving (ϕ, ψ) for the two structures are listed in Table 3. ORTEP drawings of the asymmetric units are in the Supporting Information. Additional details including atomic coordinates and anisotropic displacement parameters as well as complete lists of bond lengths, angles, and torsion angles are in CIF format available free of charge via www.ccdc.cam.ac.uk/conts/retrieving.html.

Results and Discussion

Temperature Dependence of an ^{15}N Shielding Tensor. Figure 1 shows powder spectra of AGG at 20 °C and −123 °C. The crystallographic R-factor, 0.054, of AGG is both small and representative of the peptides studied here. While there is some increase in the homogeneous line-width upon lowering the temperature by 150 °C, the overall breadth and shielding components are unchanged within spectral resolution, 4 ppm, and we conclude that, aside from averaging due to molecular vibrations, the results reported here are representative of static shielding tensors.

(37) Sheldrick, G. M. *SHELXL-97*, *Program for the Refinement of Crystal Structures*; University Göttingen: Göttingen, Germany, 1997.
(38) *SHELXTL*, *Program Library for Structure Solution and Molecular graphics*, version 6.12; Bruker Advanced X-ray Solutions, Inc.: Madison, WI, 2001.
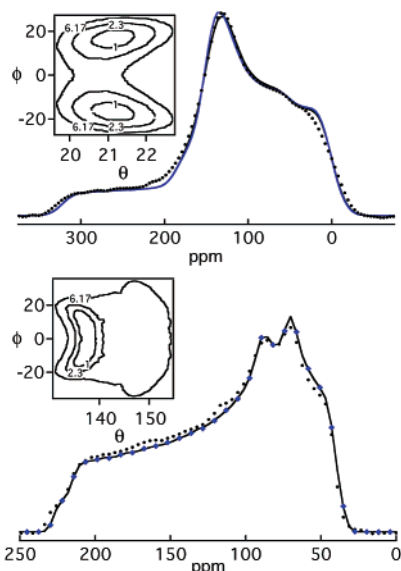
Figure 2. ^{1}H (top) and ^{13}C (bottom) coupled ^{15}N spectra of VGG. Experimental spectra are in black dots, and simulations with optimum fitting parameters, Table 2, are in black lines. Also shown, in blue, are spectrum simulations for $\phi = 0°$. Insets are contour plots of χ^2 in the region of the optimum values.

Table 1. Polar Orientations of the N−H and N−C$^\alpha$ Bonds Determined from the Dipole Coupled Spectra, Figure 2[a]

peptide	(θ_{NH}, ϕ_{NH})	$(\theta_{NC\alpha}, \phi_{NC\alpha})$
GGV[b]	20.0°(1), - - -	135°(7), - - -
GGV[a]	23.5°(1), ±31°(6)	138°(7), ±7°(13)
VGG	21.0°(1), ±15°(7)	138°(4), ±6°(13)

[a] The polar angles are relative to a frame in which the shielding tensor is diagonal (x, y, and z along δ_{33}, δ_{22}, and δ_{11}, respectively).

Shielding Tensor Orientation from Two Dipolar Couplings. Shown in Figure 2 are ^{1}H and ^{13}C coupled ^{15}N spectra of VGG which display the combined effects of ^{15}N shielding and dipolar coupling from either ^{1}H−^{15}N (top) or ^{13}C−^{15}N (bottom). Simulations shown in Figure 2 are parametrized in terms of the polar orientation, (θ,ϕ), of the N−H or N−C$^\alpha$ bonds in the orthogonal frame of the experimentally determined principal components taken from Table 2. We have used standard peptide bond lengths[39] (1.04 Å for N−H or 1.46 Å for ^{13}C$^\alpha$−^{15}N), and the Lee−Goldburg scale factor (~0.58) was treated as a fitting parameter which accounts for either a somewhat different N−H bond length[14] or a nonideal scale factor. Listed in Table 1 are the best-fit angles for VGG and two GGV polymorphs. For example, θ_{NH} is the angle between the N−H bond and δ_{11}. Furthermore, a nonzero ϕ_{NH} indicates that the N−H bond is out of the δ_{11},δ_{33} plane. The orientations and uncertainties (67% joint confidence limits from the $\chi^2 = 2.13$ contour) are shown in the insets of Figure 2. Due to inherent symmetries of the shielding and dipole interactions, the fits are not unique. Discarding (i) N−H orientations in which δ_{11} is not rotated ~20° from the N−H bond toward C′[11] and (ii) N−C$^\alpha$ orientations that are not close to the crystallographically observed H−N−C$^\alpha$ bond angle (~118°)[39] yields unique θ values but only the magnitudes of ϕ. Compared to N−C$^\alpha$, the N−H bond orientation is more accurately determined due to the larger ^{1}H−^{15}N coupling, and θ angles are better

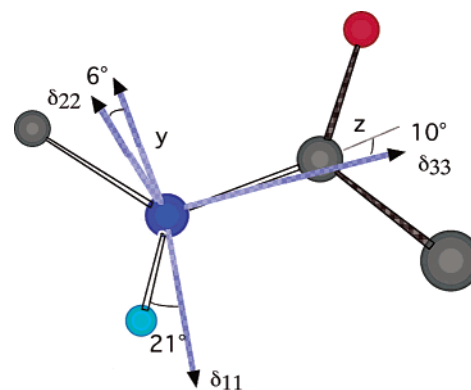(39) Voet, D.; Voet, J. G. *Biochemistry*, 2nd ed.; Wiley & Sons: New York, 1995.

Figure 3. ^{15}N shielding tensor orientations in the peptide frame. Reference axes are defined such that y is normal to the peptide plane and z is along the N−C′ bond. One of two possible orientations of the VGG tensor is shown. In the other orientation, angles are the same but δ_{22} is rotated to the other side of y and δ_{33} is below the plane. The orientation in the sheetlike GGV polymorph is similar as follows: δ_{11} is 23.5° from the N−H bond, δ_{22} is 13° from y, and δ_{33} is 14° from z.

Table 2. ^{15}N Shielding Parameters, δ_{iso}, $\delta_{span} = \delta_{11} - \delta_{33}$, and $\delta_{dev} = \delta_{22} - \delta_{33}$[a]

peptide (code)	δ_{iso} (ppm)	δ_{span} (ppm)	δ_{dev} (ppm)	Γ (ppm)
VGG (COPBIS)	113.7	176.2(2.0)	34.9(2.5)	103.9
GGG[a] (BIBRUZ)	103.2	176.4(1.8)	34.6(2.7)	104.2
GGG[b] (GLYLIB)	109.2	171.9(2.5)	20.8(4.1)	107.0
GGF (GADMIH)	108.2	169.0(5.0)	14.0(5.0)	107.7
GGG[c] (TGLYCY10)	107.7	174.8(1.4)	23.0(2.5)	108.1
GGV[a] (213477)	110.1	168.0(2.6)	28.0(5.0)	101.4
GGG[d] (GGGCAC)	116.0	161.9(3.6)	10.0(7.0)	104.4
YGG (LTYRGG)	104.8	162.8(2.4)	11.7(4.4)	104.4
GGV[b] (CUWRUH)	112.8	164.0(5.0)	7.00(5.0)	106.9
FGG (FIZWIU01)	115.9	170.2(1.7)	17.9(3.1)	107.0
PGG (FABXUB10)	106.7	157.4(1.9)	7.30(3.9)	102.4
AGG[a] (CALXES20)	104.8	161.6(2.3)	7.30(4.5)	105.2
AGG[b] (213476)	102.8	167.3(5.0)	23.3(5.0)	102.9

[a] Individual components, δ_{ii}, are related to table values, δ_{span} and δ_{dev}, by $\delta_{33} = \delta_{iso} - (\delta_{span} + \delta_{dev})/3$. Also listed is the parameter $\Gamma = (\delta_{11} - \delta_{iso})(1 - \eta^2/3)^{1/2}$ used in the analysis of relaxation experiments. Superscripts, which are used in Tables 1-4, label different polymorphs. GGG[c] has two molecules in the asymmetric unit with equivalent ^{15}N isotropic shifts at the central gly residue.

determined than ϕ angles since, in the limit of an axially symmetric shielding tensor, ϕ is arbitrary and thus undetermined. This is the case of the α-helixlike polymorph GGV[b], and only $\theta_{NH} = 20°$ is well determined. For the sheetlike peptides, GGV[a] and VGG, the N−H bonds are clearly out of the plane defined by δ_{11} and δ_{33} ($\phi_{NH} \neq 0$), while the N−C$^\alpha$ bonds, within experimental error, are in the plane.

Two possible tensor orientations are thus consistent with the data and are shown in Figure 3 relative to a molecular frame with standard peptide geometry[39] (obtained using the transformation obtained in the appendix). The important conclusion is that, to a modest degree, δ_{11} and δ_{33} do not lie in the peptide plane. These results are in agreement with both experimental observations based on N−H dipolar couplings[14,40] and theoretical calculations.[41]

Shielding Parameters in Glycyl Peptides. Isotropic chemical shifts, δ_{iso}, and the anisotropic shielding parameters, δ_{span} and δ_{dev}, are listed in Table 2 for the 13 peptides. We first consider

(40) Lee, D. K.; Wei, Y. F.; Ramamoorthy, A. *J. Phys. Chem. B* **2001**, *105*, 4752−4762.
(41) Brender, J. R.; Taylor, D. M.; Ramamoorthy, A. *J. Am. Chem. Soc.* **2001**, *123*, 914−922.

Table 3. Summary of Tripeptide Structural Data[a]

sequence	2°	charge	ψ_1 (deg)	ϕ_2 (deg)	ψ_2 (deg)	χ^1_1 (deg)	r_{HB-I} (Å)	r_{HB-D} (Å)	δ_{iso} (ppm)
VGG	sheet	zwit	123	−155	155	−53	3.05	3.05	113.7
GGG[a]	sheet	+1(HCl)	165	−153	160		absent	2.96	103.2
GGG[b]	sheet	zwit	−147	63	−141		2.81	2.95	109.2
GGF	sheet	+1(HCl)	166	64	−153		2.92	3.17	108.2
GGG[c]	ext	"		−150	178	172	2.92	2.94	107.7
"	"	"		−162	−165	175	3.13	2.99	107.7
GGV[a]	sheet	+1(HCl)	180	−159	167		2.80	2.59	110.1
GGG[d]	helix	zwit	163	−98	−3		2.40	3.33	116.0
YGG	helix	"	164	81	−12	74	absent	2.88	104.8
GGV[b]	helix	"	−156	−77	−22		2.99	2.78	112.8
FGG	helix	"	116	−90	−29	176	3.00	2.81	115.9
PGG	3₁	"	178	−71	167	32	3.20	2.84	106.7
AGG[a]	3₁	"	160	−83	169		3.00	2.93	104.8
AGG[b]	3₁	+1(HCl)	156	−98	149		2.83	3.02	102.8

[a] Different polymorphs are indicated by superscripts and correspond to CSD codes given in Table 2. Zwit = zwitterion, and HCl is the hydrogen chloride salt.

Table 4. Contributions to the Predicted Isotropic Shifts and Comparison with Experiment[a]

peptide	2°	$\delta(\psi_1,\phi_2)$	$\delta(\chi^1_1)$	δ(HB-I)	δ(HB-D)	δ_{iso}(pred)	δ_{iso}(exptl)
VGG	sheet	2.5	−0.5	3.8	1.0	111.5	113.7
GGG[a]	sheet	−1.0	0.0	0.0	1.3	105.0	103.2
GGG[b]	sheet	−3.0	0.0	5.0	1.3	108.0	109.2
GGF	sheet	−2.0	0.0	4.4	0.80	107.9	108.2
GGG[c]	ext.	−1.0	0.0	4.4	1.4	109.5	107.7
"	"	−1.0	0.0	3.5	1.2	108.4	107.7
GGV[a]	sheet	−1.0	0.0	5.0	3.7	112.4	110.1
GGG[d]	helix	2.0	0.0	5.0	3.0	117.1	116.0
YGG	helix	−2.0	−2.0	0.0	3.7	106.8	104.8
GGV[b]	helix	0.5	0.0	2.6	3.7	113.9	112.8
FGG	helix	3.5	−2.0	2.6	3.7	114.9	115.9
PGG	3₁	1.0	0.0	3.2	1.8	104.5	106.7
AGG[a]	3₁	2.0	−3.3	4.0	1.4	102.6	104.8
AGG[b]	3₁	2.0	−3.3	4.9	1.1	103.2	102.8

[a] For sheet, α-helix, and 3₁-helix residues, δ_{ref} = 104.7, 107.1, and 98.5 ppm, respectively.

the isotropic shifts for which there is a substantial empirical and theoretical understanding based on structure. Important determinants identified are the neighboring torsion angles (ψ_{i-1}, ϕ_i), to a lesser degree the adjacent angles (ϕ_{i-1}, ψ_i), the type and side chain conformation (χ^1_{i-1}) of the preceding residue, and H-bond distances (direct and indirect). These structural properties, taken from the X-ray structures, are listed in Table 3. Since the central residue of tripeptides is studied here, ϕ_1 is irrelevant and not listed.

Several comparisons are helpful in isolating individual effects. For example, GGV[b], δ_{iso}= 112.8 ppm, and FGG, δ_{iso}= 115.9 ppm, have similar helixlike torsion angles (ϕ_2, ψ_2), both direct and indirect H-bonds with nearly equivalent H-bond distances, but different ψ_1. This suggests that the shift difference of 3.1 ppm is due to conformation, ψ_1 and χ_1, and/or the type of preceding residue, G or F. Density functional calculations indicate that replacing a preceding G with F and χ_1 = 180° has little or no effect in a helix structure. To examine the effect of backbone conformation, we use empirical conformational surfaces compiled from solution NMR studies[2] since the recently described procedure[20] based on DFT calculations cannot be applied to tripeptides.[21] With ϕ_2 = −80°, varying ψ_1 from −156° (GGV[b]) to 116°(FGG) results in the 3 ppm downfield shift that is observed here. Applying these same conformational surfaces to two sheet peptides with the same preceding residue, GGG[b], δ_{iso}= 109.2 ppm, and GGF, δ_{iso}= 108.2 ppm, a small 0.5 ppm downfield conformational shift for the former is

predicted based on similar torsion angles. While both peptides have direct and indirect H-bonds, they are shorter in GGG[b] and expected to result in an additional downfield shift. Using density functional calculations for H-bonds in helices, the net downfield shift for conformation and H-bond length is 1.5 ppm; in good agreement with the 1 ppm experimental difference. The effect of H-bonds on isotropic shifts is most dramatic in GGG[a] which has no indirect H-bond and, accordingly, the most upfield shift (103.2 ppm) of the sheet residues. The most deshielded sheet residue, VGG with δ_{iso}= 113.7 ppm, has both direct and indirect H-bonds, but they are relatively long and cannot alone account for the large downfield shift. The remaining downfield shift can be parsed into two similar contributions from the backbone torsion angles and the side chain conformation ($\chi_1 \approx 180°$) of the preceding val residue.

Contributions to the observed shifts predicted in this way for the complete set are summarized in Table 3 using an additive model with five terms.

$$\delta_{obs} = \delta(\psi_1,\phi_2) + \delta(\chi^1_1) + \delta(\text{HB-I}) + \delta(\text{HB-D}) + \delta_{ref} \quad (1)$$

As above, the contribution from backbone torsions is taken from an empirical chemical shift surface,[2] while the effects of side-chain conformation, $\delta(\chi_1^1)$, and indirect and direct H-bonding, δ(HB-I) and δ(HB-D), are from the Xu and Case analysis of their DFT calculations (Table 4).[21] Also following Xu and Case, we have used different reference shifts, δ_{ref}, for different 2° structures[21] adjusted here to best fit the data. The observed shifts are reasonably well predicted indicating that the simple analysis accounts for the primary determinants and their approximate sizes.

The variation of principal components is larger than the variation of isotropic shifts, Table 2. The range for δ_{11} and δ_{33} is 16 ppm, while that for δ_{22} is 22 ppm. Moreover, shielding parameters are grouped according to their corresponding 2° structures indicating that conformation is a dominant factor in δ_{span} and δ_{dev}. Sheet and extended conformations have large δ_{span}, 169−176 ppm, and large δ_{dev}, 21−35 ppm. Helix residues have intermediate δ_{span}, 162−170 ppm, and smaller δ_{dev}, 7−18 ppm. The smallest spans are observed in 3₁ helices, 157−167 ppm, which also have small δ_{dev}, 7−23 ppm. Shielding parameters for gly in sheetlike conformations are comparable to the "average" tensor reported by Cornilescu and Bax[3] for all sheet residues in ubiquitin, δ_{span} = 174.2 ± 4 ppm and δ_{dev} =

26.2 ± 3 ppm. Their values for the "average" helix parameters, $\delta_{span} = 170.7 \pm 6$ ppm and $\delta_{dev} = 9.6 \pm 4$ ppm, are also comparable albeit a somewhat smaller δ_{span}.

Concluding Remarks

Accurate knowledge of ^{15}N chemical shielding parameters is essential to a wide variety of solution and solid-state NMR experiments. A library of these parameters obtained from structurally characterized tripeptides shows systematic trends in glycyl isotropic shifts, tensor spans, and their deviations from axial symmetry. Tensor spans, for example, are found to vary over a large range, 157.4 ppm to 176.4 ppm, and low temperature experiments confirm that these are representative of static values. While this library is limited to glycine, the ranges of shielding parameters are comparable to those determined for other amino acids in both peptides and the average tensor measured in a weakly oriented protein.[11,12,14−19]

We have used two dipolar couplings, ^{1}H$-^{15}$N and ^{13}C$^{\alpha}-$ ^{15}N, to orient the shielding tensor relative to the peptide plane. Based on the ^{1}H$-^{15}$N coupling, the angle between δ_{11} and the N$-$H bond, θ_{NH}, is accurately determined ($\pm 1°$) and is in the range previously seen, 20−25°. While it is frequently assumed that the δ_{11}, δ_{33} shielding tensor and peptide planes are coincident, this is not confirmed here. Based on the ^{1}H$-^{15}$N coupling in *N*-acetylglycine, a similar conclusion was reported previously.[14] The orientation, pictured in Figure 3 and derived in the appendix, is not unique and somewhat imprecise. That two orientations are consistent with experiment is an inherent ambiguity of the approach based on dipolar couplings and the lack of precision results from the fact that ^{15}N amide tensors typically have small δ_{dev}. We anticipate that the correct choice of the two possibilities given here could be made with ab initio shielding tensor calculations.[41,42] Alternatively, a modest number of single-crystal tensor determinations in addition to that of gly-gly·HCl[11] would be quite useful.

Isotropic ^{15}N glycyl shifts in the 13 peptides vary from 102.8 to 116.0 ppm, i.e., a substantial fraction of the range seen in proteins. Notably, the range in the sheetlike structures examined is nearly as large. An additive model appropriate for tripeptides based on contributions from the nearest backbone torsion angles, the previous residue and its side-chain conformation, indirect H-bonding to C=O, and direct H-bonding to N$-$H is used. There is good agreement with experiment using empirically determined reference shifts for α, β, and 3_1-helix structures, as suggested by a recent DFT based procedure for calculating protein chemical shifts.[21] This indicates the general relevance

(42) Shekar, S. C.; Ramamoorthy, A.; Wittebort, R. J. *J. Magn. Reson.* **2002**, *155*, 257−262.

Table 5. Identification of 2° Structure Based on Glycyl ^{13}C$^{\alpha}$ and ^{15}N Shielding

2°	δ_{span}, ^{13}C$^{\alpha}$ (ppm)	$\delta_{dev}/\delta_{span}$, ^{13}C$^{\alpha}$	δ_{dev}, ^{15}N (ppm)
α-helix	32−45	0.25−0.40	<20
β-sheet	24−58	0.35−0.90	>20
3_1-helix	45−55	0.35−0.55	<20

of solid-state NMR studies of peptides for understanding the structural basis of chemical shielding in proteins.

Chemical shielding parameters reported here are found to have two useful properties: (i) they vary over a fairly large range (19 ppm for δ_{span} and 28 ppm for δ_{dev}) and (ii) both δ_{span} and δ_{dev} are grouped according to 2° structure. The latter feature, distinct from that seen for δ_{iso}, is particularly notable for δ_{dev}. For example, the three β-sheet or extended polymorphs of GGG have $\delta_{dev} = 21-35$ ppm, while the α-helical form has $\delta_{dev} = 10$ ppm. Similarly, the β-sheet polymorph, GGV^a, has $\delta_{dev} = 28$ ppm and the α-helical form, GGV^b, has $\delta_{dev} = 7$ ppm. We anticipate that a quantitative quantum chemical model for predicting and understanding the structural basis of these results is possible and such a model would be useful in solid-state structure determination. More immediately, these results are useful for qualitative identification of the 2° structure. Previously we identified that glycyl ^{13}C$^{\alpha}$ shielding parameters are useful for distinguishing α and 3_1 helices based on δ_{span} (32−50 ppm and 45−55 ppm, respectively) and $\delta_{dev}/\delta_{span}$ (0.25−0.4 and 0.35−0.45, respectively). Identification of β structure, which has a wide range of δ_{span} (24−58 ppm) and $\delta_{dev}/\delta_{span}$ (0.35− 0.90), is more difficult. This ambiguity is resolved with the addition of ^{15}N shielding, in particular the value of δ_{dev}. These constraints are summarized in Table 5.

Supporting Information Available: The appendix includes a derivation of the molecular orientations of the 15N tensors in a standard peptide frame using the data of Table 2 and Supporting Information reported for the X-ray structures. Included are ORTEP diagrams and CIF files for GGV·HCl (CCDC Code 213477) and AGG·HCl (CCDC Code 213476). This material is available free of charge via the Internet at http://pubs.acs.org.

JA0370342